HUMANOID TRAJECTORY GENERATION: AN ITERATIVE APPROACH BASED ON MOVEMENT AND ANGULAR MOMENTUM CRITERIA*

NIRUT NAKSUK
YONGGUO MEI
C. S. GEORGE LEE

School of Electrical and Computer Engineering, Purdue University
West Lafayette, IN 47906, USA
{*naksuk, ymei, csglee*}*@purdue.edu*

Recently, data from human walking suggest that angular momentum at the Center of Mass (CM) is highly regulated throughout the gait cycles. In this paper, we propose a humanoid robot trajectory generation that minimizes angular momentum at the CM while maintaining the humanoid robot balance. An initial humanoid robot trajectory was generated from a joint-space interpolation of the desired snapshots. Then, we apply an iterative adaptation scheme to adjust this initial trajectory to satisfy the balance as well as the angular momentum criteria. Utilization of the initial solution derived from the desired snapshots usually results in less computation required for the trajectory adaptation because the initial solution is close to the final solution if the appropriated snapshots were used. Moreover, the posture of the desired snapshots is likely to be maintained after the trajectory adaptation process. Numerical simulation was conducted to verify the validity of the proposed trajectory generation method.

Keywords: Humanoid; Trajectory Generation; Angular Momentum.

1. Introduction

Development of humanoid robots with natural and efficient movements presents many challenging problems in the humanoid locomotion research community. Existing humanoid robots such as Honda Motor's ASIMO, Sony's SDR-4X II, AIST's HRP2, and Toyota Motor's PARTNER have shown impressive abilities to walk on an even/uneven terrain or up/down stairs, nevertheless their movements are noticeably different from human's natural walk. Generally, Humanoid robot trajectory generation is an essential component in humanoid robot control. Trajectory generation requires computation of joint trajectory to fulfill a stable humanoid robot movement. Several techniques [1, 2, 3, 4, 5, 6, 7, 8, 9] were proposed to compute the joint trajectory solution resulting in different stable movements.

Early attempts to compute a joint trajectory solution utilized reduced-order humanoid robot models [1, 2, 3]. Miura and Shimoyama [1] first adopted the ZMP [10] criterion for generating balance humanoid movements. Zheng and Shen [2] derived stable humanoid robot movement for climbing up a small slope, and the CM static stability criterion was used in their work. Kajita [3] developed an inverted pendulum model to generate a balance biped

*This work was supported in part by the National Science Foundation under Grant IIS-0427260.

walking. More complete humanoid-robot model has been used in the realization of humanoid robot movement by Yamaguchi *et al.* [4,5] and Lim *et al.* [9]. In their work, trajectories of both legs were preplanned from the desired foot trajectory, then the upper-body joint trajectories were computed such that the resultant upper-body movement generates moment that maintains the whole-body balance.

Beside the effect of force/moment resulted from its own motion, the ground reaction force also plays an important role in humanoid stability. To improve the stability under the influence of ground reaction force, Fujimoto and Kawamura [6] addressed this problem by incorporating ZMP into the control loop to maintain the desired ZMP trajectory under the effect of ground reaction force. An iterative search algorithm was also introduced to deal with the whole-body humanoid robot movement. Nagasaka, *et al.* [7] used a gradient-search algorithm to produce a stable humanoid-robot movement by adjusting an initial unbalance solution into a balance whole-body movement. Huang, *et al.* [8] developed an algorithm to produce humanoid-robot movement with maximum ZMP stability margin. This is accomplished by iteratively adjusting the relative location of the hip with respect to the location of the supporting foot.

Our goal is to develop an effective scheme to generate a balance humanoid robot trajectory that produces more natural movement. In this paper, we investigate a humanoid robot trajectory generation scheme that maintains balance based on the ZMP criterion as well as minimizes the angular momentum at CM to obtain natural movement. The angular momentum criterion utilized here follows the recent investigation of human walking by Popovic, *et al.* [11]. Popovic, *et al.* suggested that the angular momentum at the human CM is highly regulated throughout the human gait cycles. The proposed scheme provides fast computation of humanoid robot movement through a concept of movement snapshots. An original solution of the humanoid robot movement was generated from a spline interpolation of the desired snapshots in the joint space. Later, this interpolated trajectory is iteratively adapted to satisfy the balance and angular momentum criteria. Since the joint solution was originally generated from the desired snapshots, it is generally observed that a movement similar to the desired snapshots is obtained. Even though all link masses of the humanoid robot are used in the computation, the proposed scheme involves less computation since the trajectory is not generated from scratch but rather from the well defined via-point representation. Moreover, the adaptation could be small if an appropriate design of the snapshots is utilized.

The organization of this paper is as follows. In Section 2, we discuss a balance constraint based on maximum moment withstandable by the humanoid robot foot and the angular momentum criterion. In Section 3, we discuss the proposed trajectory generation based on minimizing angular momentum at the humanoid robot CM and the balance criterion. The simulation results to verify the proposed trajectory generation approach are presented and discussed in Section 4. Section 5 summarizes the conclusion.

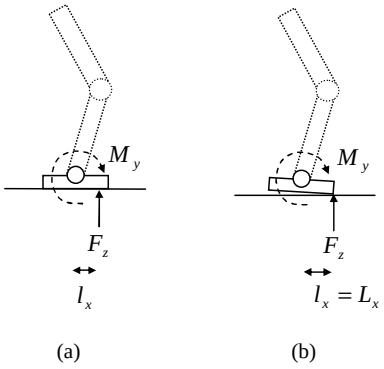

Fig. 1. (a) Humanoid robot foot contact is stable. (b) Humanoid robot starts to fall down.

2. Balance and Angular Momentum Criteria for Humanoid Locomotion

In this section, we investigate two criteria that will be utilized to generate a humanoid robot trajectory. These two criteria are the balance criterion based on the moment at the contact foot, and the angular momentum criterion. In Fig. 1(a) and (b), F_z, M_y, l_x and L_x denote the ground reaction force, moment, location of the ground reaction force and the length from the foot center to its tip, respectively. Consider the force and moment at the humanoid robot foot contact, the relation between the ground reaction force and the moment is written as

$$\frac{-M_y}{F_z} = l_x < L_x \tag{1}$$

To keep a humanoid robot from falling down on the edge of its foot, the moment applied to the foot contact from the upper-body movement and the gravitational force must not exceed the maximum withstandable moment $F_z L_x$. Thus, the condition $l_x < L_x$ must be maintained for a humanoid robot to be stable, and l_x is referred to as the ZMP in [10]. F_z, M_y are the force and moment generated by the humanoid robot movement and the gravitational force, respectively, which can be written as follows,

$$F_z = \sum_{i=1}^{N} m_i(\ddot{z}_i + g) \tag{2}$$

$$M_y = -\sum_{i=1}^{N} m_i(\ddot{z}_i + g)x_i + \sum_{i=1}^{N} m_i \ddot{x}_i z_i \tag{3}$$

where $[x, y, z]^T$ and $[\ddot{x}, \ddot{y}, \ddot{z}]^T$ are position and acceleration vectors of link i respectively. These vectors are defined with respect to the humanoid robot ankle location. N indicates the number of links, m_i is the mass of link i, and g denotes the gravitational acceleration. Thus, Eq. (1) implies that for a humanoid robot to maintain its stability, its ZMP must be within the foot supporting area. Therefore, the joint solution of a stable humanoid robot

trajectory generation must produce the desired limb movements to satisfy the above criterion. For a robot not to start falling down, M_y must be in between M_{b1} and M_{b2}. Note that for positive l_x, posture F_z results in negative moment at the robot ankle, thus

$$M_{b1} < -M_y < M_{b2} \tag{4}$$

$$-L_1 F_z < -M_y < L_2 F_z \tag{5}$$

$$-L_1 < \frac{-M_y}{F_z} < L_2 \tag{6}$$

$$-L_1 < \frac{\sum_{i=1}^{N} m_i(\ddot{z}_i + g)x_i - \sum_{i=1}^{N} m_i \ddot{x}_i z_i}{\sum_{i=1}^{N} m_i(\ddot{z}_i + g)} < L_2 \tag{7}$$

where L_1 and L_2 are the distances from the humanoid robot ankle to its heel and to its toes respectively. By utilizing the notation of the ZMP, Eq. (7) can be written as,

$$-L_1 < ZMP_x < L_2 \tag{8}$$

Beside being stable, a human also maintains his/her body angular momentum while moving. Recently, data from human walking suggest that angular momentum is highly regulated throughout the gait cycles. In walking, it was observed that angular momentum at the center of mass per weight, height and velocity is highly regulated[11]. Its value is less than 0.02 throughout human walking cycles[11]. We extend the angular momentum to humanoid robot movement.

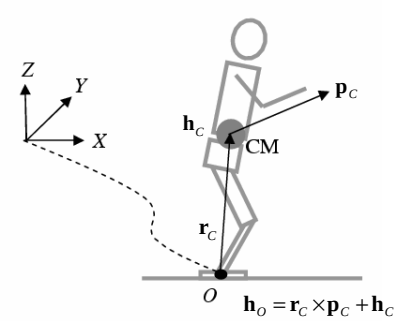

Fig. 2. Angular momentum at a fixed point O and at CM.

From Fig. 2, $\mathbf{h}_O$ denotes the angular momentum at the center of a supporting foot and can be written as

$$\begin{aligned} \mathbf{h}_O &= \mathbf{r}_C \times \mathbf{p}_C + \mathbf{h}_C \\ &= \sum_{i=1}^{N} \mathbf{r}_i \times m_i \mathbf{v}_i \end{aligned} \tag{9}$$

where $\mathbf{r}_i$, $\mathbf{v}_i$ and $\mathbf{r}_C$ are the location and the velocity of mass i, and the location of robot CM, respectively. $\mathbf{r}_C$ is found to be

$$\mathbf{r}_C = \frac{\sum_{i=1}^{N} m_i \mathbf{r}_i}{\sum_{i=1}^{N} m_i}, \tag{10}$$

$\mathbf{p}_C$ can be considered as the rate of change of $\mathbf{r}_C$ times the robot mass,

$$\mathbf{p}_C = \sum_{i=1}^{N} m_i \mathbf{v}_i \tag{11}$$

and $\mathbf{h}_C$ is the angular momentum at the CM.

3. Trajectory Generation

In this section, we discuss the proposed trajectory generation scheme. The humanoid robot trajectory is initially generated from the interpolation of the desired snapshots. The proposed adaptation scheme then adjusts the trajectory to satisfy the balance criterion as well as maintain small angular momentum at the humanoid robot CM.

3.1. *Initial Humanoid Robot Trajectory from the Desired Snapshots*

In this subsection, we discuss the generation of initial humanoid robot trajectory using an idea of movement snapshots. Snapshots are the desired discrete postures. An example of 3 consecutive desired snapshots for walking is shown in Fig. 3. These snapshots are first converted into a via-point representation in joint space. The spline interpolation is then applied to these points resulting in an initial humanoid robot trajectory of the desired movement. The process is illustrated in Fig. 3. This initial trajectory, when applied to a humanoid robot, generally results in an unbalance movement. Thus further adaptation of this initial trajectory to satisfy the balance constraint and overall body movement is required. This trajectory adaptation is discussed in the next subsection.

3.2. *Balance Criterion*

In this subsection, the adaptation of the initial trajectory to satisfy the balance criterion is discussed. Consider the moment generated by the ground reaction force as shown in Fig. 1(a). This moment can be written as an inner product of two vectors,

$$-M_y = \sum_{i=1}^{N} m_i(\ddot{z}_i + g)x_i - \sum_{i=1}^{N} m_i \ddot{x}_i z_i = \mathbf{w}^T \mathbf{u} \tag{12}$$

where (x_i, y_i, z_i) represents the mass location of link i with respect to the frame O, $\mathbf{w}$ denotes a vector of robot mass, and $\mathbf{u}$ denotes a functional vector of the robot movement. $\mathbf{w}$ and $\mathbf{u}$ are written as

$$\mathbf{w} = [m_1, \ldots, m_N]^T \tag{13}$$

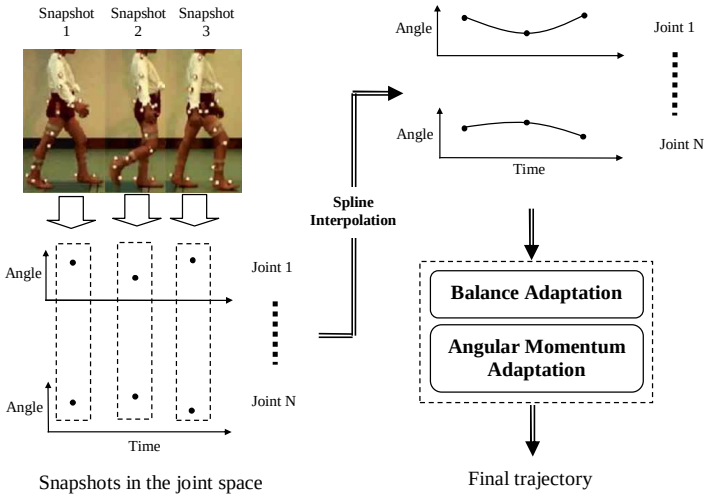

Fig. 3. Overview of the proposed trajectory generation.

$$\mathbf{u} = \begin{bmatrix} (\ddot{z}_1 + g)x_1 - \ddot{x}_1 z_1 \\ \vdots \\ (\ddot{z}_N + g)x_N - \ddot{x}_N z_N \end{bmatrix} \tag{14}$$

The moment $-M_y$ must be within the bounds of M_{b1} and M_{b2} as described in Eq. (4) for a humanoid robot to be stable. Thus, the moment bounds for a balance trajectory can be written as

$$M_{b1} = -L_1 \sum_{i=1}^{N} m_i(\ddot{z}_i + g) = -L_1 \mathbf{w}^T \mathbf{u}_{low} \tag{15}$$

$$M_{b2} = L_2 \sum_{i=1}^{N} m_i(\ddot{z}_i + g) = L_2 \mathbf{w}^T \mathbf{u}_{up} \tag{16}$$

where L_1 and L_2 are the distances from the humanoid robot ankle to its heel and its toes respectively. $\mathbf{u}_{up}$ and $\mathbf{u}_{low}$ represent the upper and the lower bounds of $\mathbf{u}$, respectively. Thus, the constraint is written as

$$M_{b1} < \mathbf{w}^T \mathbf{u} < M_{b2} \tag{17}$$

An adjustment of the vector $\mathbf{u}$ is required to move M_y into the defined boundary. The change in $\mathbf{u}$ to move M_y inside the boundary can be computed as follows,

$$\delta\mathbf{u} = \alpha \frac{\mathbf{w}\mathbf{w}^T}{\mathbf{w}^T\mathbf{w}} \Delta\mathbf{u} = \begin{cases} \alpha \frac{\mathbf{w}\mathbf{w}^T}{\mathbf{w}^T\mathbf{w}} (\mathbf{u}_{up} - \mathbf{u}) & \text{if } \mathbf{w}^T\mathbf{u} > M_{b2} \\ \alpha \frac{\mathbf{w}\mathbf{w}^T}{\mathbf{w}^T\mathbf{w}} (\mathbf{u}_{low} - \mathbf{u}) & \text{if } \mathbf{w}^T\mathbf{u} < M_{b1} \end{cases} \tag{18}$$

where α is a small positive constant. $\frac{\mathbf{w}\mathbf{w}^T}{\mathbf{w}^T\mathbf{w}}$ projects $\Delta\mathbf{u}$ onto a space spanned by $\mathbf{w}$. The trajectory adaptation is illustrated in Fig. 4.

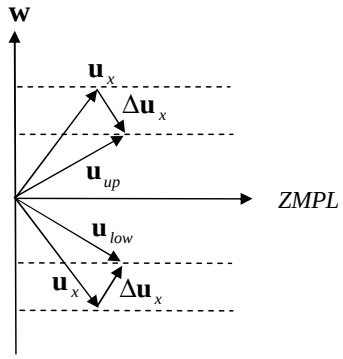

Fig. 4. Diagram of the moment adaptation.

Based on the change in the functional vector $\mathbf{u}$ represented by $\delta\mathbf{u}$, we now describe the corresponding change in the humanoid robot movement. In this paper, we only derive the movement adjustment in the x direction. The movement adjustment in the other directions can be done in the similar way. To compute $\delta\mathbf{x}$, the acceleration of each mass component can be approximated as,

$$\ddot{\mathbf{r}}_i^{\,k} \simeq \frac{\mathbf{r}_i^{k+1} - 2\mathbf{r}_i^k + \mathbf{r}_i^{k-1}}{(\Delta T)^2}, \tag{19}$$

where $\mathbf{r}_i^k$ represents a position vector $\mathbf{r}$ from O to the mass location of link i at the time step k. Based on $\mathbf{u}$ defined in Eq. (14), the component u_x^k of $\mathbf{u}$ at time step k can be written in terms of x^k as follows,

$$u_x^k = -\frac{z^k}{(\Delta T)^2}x^{k-1} + \left(\left(\dot{z}^k + g\right) + 2\frac{z^k}{(\Delta T)^2}\right)x^k - \frac{z^k}{(\Delta T)^2}x^{k+1} \tag{20}$$

or

$$u_x^k = a^k x^{k-1} + b^k x^k + a^k x^{k+1} \tag{21}$$

For each link i, we arrange u_x^k from k = 1 to K to obtain the following expression

$$\begin{bmatrix} u_x^1 \\ u_x^2 \\ \vdots \\ u_x^{K-1} \\ u_x^K \end{bmatrix}_i = \begin{bmatrix} b^1 & a^1 & 0 & 0 & \dots & \dots & 0 \\ a^2 & b^2 & a^2 & 0 & \dots & \dots & 0 \\ \vdots & \vdots & \vdots & \vdots & \vdots & \vdots & \vdots \\ 0 & \dots & \dots & 0 & a^{K-1} & b^{K-1} & a^{K-1} \\ 0 & \dots & \dots & 0 & 0 & a^K & b^K \end{bmatrix}_i \begin{bmatrix} x^1 \\ x^2 \\ \vdots \\ x^{K-1} \\ x^K \end{bmatrix}_i + \begin{bmatrix} a^1 x^0 \\ 0 \\ \vdots \\ 0 \\ a^K x^{K+1} \end{bmatrix}_i \tag{22}$$

To solve for the robot trajectory of link i denoted as $\mathbf{x}_i$, Eq. (22) can be written as,

$$\begin{aligned} \mathbf{u}_i &= \mathbf{A}_i \mathbf{x}_i + \mathbf{b}_i \\ \delta \mathbf{u}_i &= \mathbf{A}_i \delta \mathbf{x}_i \\ \delta \mathbf{x}_i &= \mathbf{A}_i^{\dagger} \delta \mathbf{u}_i \end{aligned} \tag{23}$$

where $\mathbf{A}_i^{\dagger}\ \mathbf{A}_i = \mathbf{I}$. After repeating Eq. (23) for all link i, we can update the humanoid robot trajectory $\boldsymbol{\theta}^j$ as

$$\boldsymbol{\theta}^{j+1} = \boldsymbol{\theta}^j + \mathbf{J}^{\dagger} \delta \mathbf{x}_u \tag{24}$$

where $\delta \mathbf{x}_u = [\delta \mathbf{x}_1, ..., \delta \mathbf{x}_N]^T$ represents the deviation of the humanoid robot trajectory $\mathbf{x}$ as contributed by $\delta \mathbf{u}$ to satisfy the balance criterion. $\mathbf{J}$ is a Jacobian matrix in the x direction, and $\mathbf{J}^{\dagger}$ represents the pseudo inverse of $\mathbf{J}$.

3.3. *Momentum Criterion*

In this subsection, we further adjust the robot trajectory to minimize the robot angular momentum at the CM such that its value is within a desirable boundary. This can be realized by moving $\mathbf{h}_O$ toward $\mathbf{r}_C \times \mathbf{p}_C$ whenever $\mathbf{h}_O$ is deviated from the desirable boundary.

First, we denote the angular momentum at the center of the supporting foot $\mathbf{h}_O$ as

$$\mathbf{h}_O = [h_{Ox}, h_{Oy}, h_{Oz}]^T. \tag{25}$$

From Eq. (9), each component of $\mathbf{h}_O$ can be written as an inner product of two vectors as,

$$h_{Ox} = \sum_{i=1}^{N} m_i (y_i \dot{z}_i - z_i \dot{y}_i) = \mathbf{w}^T \mathbf{v}_x \tag{26}$$

$$h_{Oy} = \sum_{i=1}^{N} m_i (-x_i \dot{z}_i + z_i \dot{x}_i) = \mathbf{w}^T \mathbf{v}_y \tag{27}$$

$$h_{Oz} = \sum_{i=1}^{N} m_i (x_i \dot{y}_i - y_i \dot{x}_i) = \mathbf{w}^T \mathbf{v}_z \tag{28}$$

where $\mathbf{w}$, $\mathbf{v}_x$, $\mathbf{v}_y$ and $\mathbf{v}_z$ are denoted as

$$\mathbf{w} = \left[m_1, \ldots, m_N \right]^T \tag{29}$$

$$\mathbf{v}_x = \left[(y_1 \dot{z}_1 - z_1 \dot{y}_1), \ldots, (y_N \dot{z}_N - z_N \dot{y}_N) \right]^T \tag{30}$$

$$\mathbf{v}_y = \left[(-x_1 \dot{z}_1 + z_1 \dot{x}_1), \ldots, (-x_N \dot{z}_N + z_N \dot{x}_N) \right]^T \tag{31}$$

$$\mathbf{v}_z = \left[(x_1 \dot{x}_1 - x_1 \dot{y}_1), \ldots, (x_N \dot{y}_N - x_N \dot{y}_N) \right]^T \tag{32}$$

To move $\mathbf{h}_O$ toward $\mathbf{r}_C \times \mathbf{p}_C$, we first write $\mathbf{r}_C \times \mathbf{p}_C$ in terms of $\mathbf{w}$, $\mathbf{s}_x$, $\mathbf{s}_y$ and $\mathbf{s}_z$ as,

$$\mathbf{r}_C \times \mathbf{p}_C = \begin{bmatrix} \mathbf{w}^T \mathbf{s}_x \\ \mathbf{w}^T \mathbf{s}_y \\ \mathbf{w}^T \mathbf{s}_z \end{bmatrix} \tag{33}$$

Without loss of generality, let us consider only the angular momentum adaptation on the sagittal plane or about the y-axis. From Eq. (33), the boundary of $\mathbf{s}_y$ represented by $\mathbf{s}_y^+$ and $\mathbf{s}_y^-$ can be computed as,

$$\mathbf{s}_y^+ = \frac{\mathbf{w}}{\mathbf{w}^T\mathbf{w}}([\mathbf{r}_C \times \mathbf{p}_C]_y + b) \tag{34}$$

$$\mathbf{s}_y^- = \frac{\mathbf{w}}{\mathbf{w}^T\mathbf{w}}([\mathbf{r}_C \times \mathbf{p}_C]_y - b) \tag{35}$$

where $[*]_y$ denotes the y component of $*$. Whenever $\mathbf{h}_O$ is outside the desired boundary of $\pm b$ centering at $\mathbf{r}_C \times \mathbf{p}_C$, where $b = h_C * \text{weight} * \text{height} * \text{velocity}$, and h_C is a normalized angular momentum at CM, the robot movement is adapted to move $\mathbf{h}_O$ closer to $\mathbf{r}_C \times \mathbf{p}_C$ such that it is within the desired boundary. Thus, to move h_{Oy} to be within the vicinity of $[\mathbf{r}_C \times \mathbf{p}_C]_y \pm b$, the following update rule is applied,

$$\delta\mathbf{v}_y = \alpha\Delta\mathbf{v}_y = \begin{cases} \alpha\frac{\mathbf{w}\mathbf{w}^T}{\mathbf{w}^T\mathbf{w}}(\mathbf{s}_y^+ - \mathbf{v}_y) & \text{if } \mathbf{w}^T\mathbf{v} > \mathbf{w}^T\mathbf{s}_y^+ \\ \\ \alpha\frac{\mathbf{w}\mathbf{w}^T}{\mathbf{w}^T\mathbf{w}}(\mathbf{s}_y^- - \mathbf{v}_y) & \text{if } \mathbf{w}^T\mathbf{v} < \mathbf{w}^T\mathbf{s}_y^- \end{cases} \tag{36}$$

where α is a small positive constant that allows the process to converge. $\delta\mathbf{v}_x$ and $\delta\mathbf{v}_z$ can be computed in the similar way. This adaptation process is illustrated in Fig. (5).

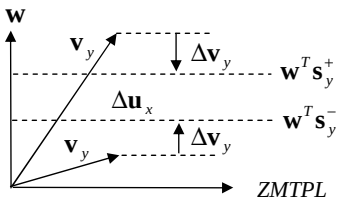

Fig. 5. Diagram of momentum projection.

We now derive the adjustment in the robot trajectory $\delta\boldsymbol{\theta}$ based on the derived $\delta\mathbf{v}$. First, the velocity of each mass component of the humanoid robot is approximated as,

$$\dot{\mathbf{r}_i}^k \simeq \frac{\mathbf{r}_i^{k+1} - \mathbf{r}_i^k}{\Delta T} \tag{37}$$

where $\mathbf{r}_i^k$ represents a vector $\mathbf{r}_i$ from point O to the center of mass i at time step k, and ΔT represents the sampling period. Consider adjusting the horizontal movement to satisfy $\delta\mathbf{v}_y$, the component v_y^k of $\mathbf{v}_y$ at time step k can be written in terms of x^k as

$$v_y^k = a^k x^{k-1} + b^k x^k \tag{38}$$

where $a^k = -\dot{z} - \frac{z^k}{\Delta T}$ and $b^k = \frac{z^k}{\Delta T}$. For each link i, we arrange v_x^k from time step k = 1

to K to obtain the following,

$$\begin{bmatrix} v_y^1 \\ v_y^2 \\ \vdots \\ v_y^{K-1} \\ v_y^K \end{bmatrix}_i = \begin{bmatrix} a^1 & b^1 & 0 & 0 & \dots & \dots & 0 \\ 0 & a^2 & b^2 & 0 & \dots & \dots & 0 \\ \vdots & \vdots & \vdots & \vdots & \vdots & \vdots & \vdots \\ 0 & \dots & \dots & 0 & 0 & a^{K-1} & b^{K-1} \\ 0 & \dots & \dots & 0 & 0 & 0 & a^K \end{bmatrix}_i \begin{bmatrix} x^1 \\ x^2 \\ \vdots \\ x^{K-1} \\ x^K \end{bmatrix}_i + \begin{bmatrix} 0 \\ 0 \\ \vdots \\ 0 \\ b^K x^{K+1} \end{bmatrix}_i \tag{39}$$

To solve for the robot trajectory of link i denoted as $\mathbf{x}_i$, Eq. (39) can be written as,

$$\begin{aligned} \mathbf{v}_i &= \mathbf{A}_i \mathbf{x}_i + \mathbf{b}_i \\ \delta \mathbf{v}_i &= \mathbf{A}_i \delta \mathbf{x}_i \\ \delta \mathbf{x}_i &= \mathbf{A}_i^\dagger \delta \mathbf{v}_i \end{aligned} \tag{40}$$

where $\mathbf{A}_i^\dagger \mathbf{A}_i = \mathbf{I}$. After repeating Eq. (40) for each link i, the humanoid robot trajectory $\boldsymbol{\theta}$ can be updated as

$$\boldsymbol{\theta}^{j+1} = \boldsymbol{\theta}^j + \mathbf{J}^\dagger \delta \mathbf{x}_v \tag{41}$$

where $\delta \mathbf{x}_v = [\delta \mathbf{x}_1, ..., \delta \mathbf{x}_N]^T$ represents the deviation of the humanoid robot movement $\mathbf{x}$ as contributed by $\delta \mathbf{v}$ to satisfy the angular momentum criterion. $\mathbf{J}$ is a Jacobian matrix in the x direction, and $\mathbf{J}^\dagger$ represents the pseudo inverse of $\mathbf{J}$.

Figure 6 summarizes the process of the proposed humanoid robot trajectory generation. The proposed scheme iteratively adjusts the robot trajectory $\boldsymbol{\theta}$ by $\mathbf{J}^\dagger \delta \mathbf{x}_u$ and $\mathbf{J}^\dagger \delta \mathbf{x}_v$. We have realized the trajectory adaptation by constructing the functional vectors in terms of the robot trajectory. The functional vector $\mathbf{u}$ is constructed from the moment at the robot supporting foot while the functional vector $\mathbf{v}$ is constructed for the angular momentum. Projection of $\mathbf{u}$ onto $\mathbf{w}$ produces the moment acting at the robot foot that directly influences the humanoid robot balance. The projection of $\mathbf{v}$, on the other hand, produces the angular momentum at the robot's CM. These two vectors reside in the same vector space as the mass distribution vector $\mathbf{w}$. Throughout the iterations, both $\mathbf{u}$ and $\mathbf{v}$ are adjusted in the direction of $\mathbf{w}$ through the projection matrix $\frac{\mathbf{w}\mathbf{w}^T}{\mathbf{w}^T\mathbf{w}}$. This adjustment results in changes of moment and angular momentum. Although both $\mathbf{u}$ and $\mathbf{v}$ are adapted in the same direction, they induce different movements. Beside projecting $\mathbf{u}$ or $\mathbf{v}$ onto $\mathbf{w}$, projecting these vectors onto a plane that is orthogonal to $\mathbf{w}$ denoted by $ZMPL$ in Fig. 4 resulting in movement that generates zero moment at the center of the contact foot, or zero angular momentum at CM in the case of $\mathbf{v}$. The projection onto $ZMTPL$ in Fig. 5 can be extended to the trajectory generation during the flight phase in running, which requires movement with zero angular momentum at the CM.

4. Computer Simulations

Computer simulations were performed to evaluate the proposed trajectory generation. We used a humanoid robot model that is composed of 11 masses including head, body, hip, two upper/lower arms, and two upper/lower legs. This model is shown in Fig. 7(a). The weights of all the components are shown in Table 1. All the masses are assumed to be point

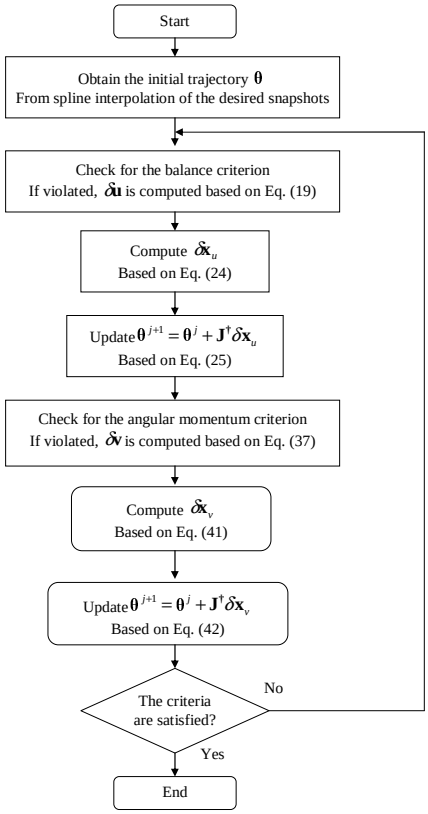

Fig. 6. Flow diagram of the proposed trajectory generation scheme.

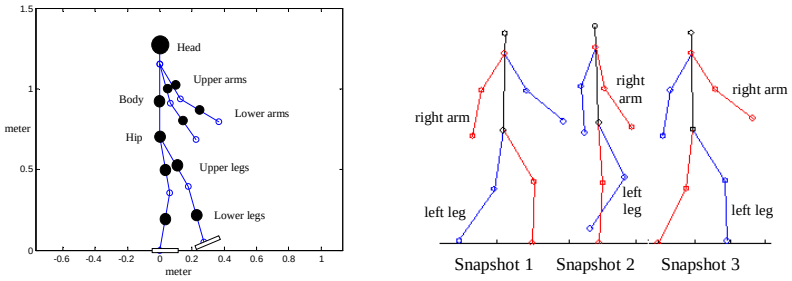

(a) (b)

Fig. 7. (a) Humanoid robot model. (b) Snapshots used in a walking simulation .

masses and located at the center of the corresponding links. We first created an initial walking trajectory from a spline interpolation in the joint space of three desired snapshots such that the humanoid robot walked at a speed of one step per second. These desired snap-

Table 1. Weight of the components of a humanoid robot model.

Links	Head	Body	Hip	Upper arm	Lower arm	Upper leg	Lower leg
Mass (kg)	3	30	27	0.6	0.6	5.1	7

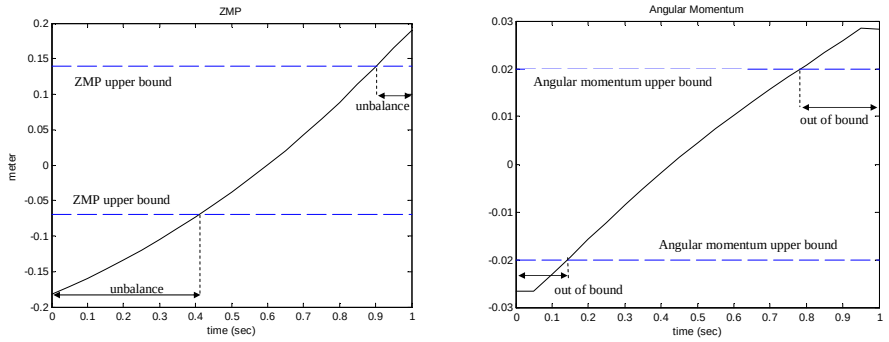

(a) (b)

Fig. 8. (a) ZMP of the initial humanoid robot trajectory. (b) Angular momentum of the initial humanoid robot trajectory.

shots are shown in Fig. 7(b). The ZMP and the normalized angular momentum at CM of the humanoid robot were computed from the initial trajectory and shown in Fig. 8(a) and (b), respectively. The upper bound and lower bound of the ZMP are the distances from the center of frame O defined in Fig. 1 to the tip of the humanoid robot foot and the humanoid robot heel. These values are 14 cm and 7 cm, respectively. The upper bound and the lower bound of the ZMP define a stable boundary for the humanoid robot to stay balanced. As expected, the initial humanoid robot trajectory resulted in the ZMP being outside the stable boundary as well as the angular momentum at the CM being outside the desired boundary defined by $\pm b$. We adopted the value of 0.02 similar to what has been observed in human walking[11]. Figure 9 shows the adaptation of the humanoid robot ZMP throughout the iterations. The initial trajectory results in the ZMP of the humanoid robot being outside the stability boundary depicted in the figure. After applying the proposed trajectory adjustment for 40 iterations, the ZMP of the final iteration stayed within the stable ZMP boundary. Similarly, the adaptation of the angular momentum at the humanoid robot CM from the initial trajectory is shown in Fig. 9. After 40 iterations, the final trajectory resulted in the normalized angular momentum of the humanoid robot being within the desired boundary of ± 0.02. The humanoid robot movement as a result of the final trajectory generated from the proposed approach is depicted in Fig. 10.

5. Conclusions

We have presented a trajectory generation scheme based on an iterative computational approach that produces a balance humanoid robot trajectory. The resultant humanoid robot

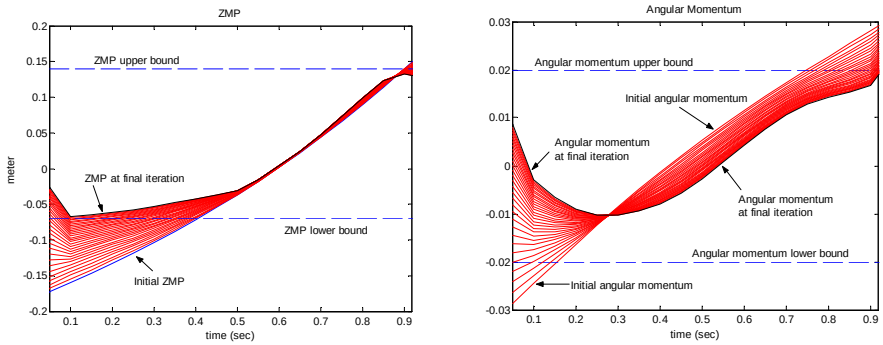

(a) (b)

Fig. 9. (a) ZMP in the x direction. (b) Angular Momentum at CM per mass, height and speed of the humanoid robot.

trajectory satisfies the balance constraint as well as maintains the angular momentum at the humanoid robot CM within the desired boundary. The utilization of an initial humanoid robot trajectory from the spline interpolation of the desired snapshots, as well as the iterative adaptation resulted in reducing the computational burdens since the trajectory was not created from sketch. Since the snapshots can be chosen arbitrarily, the proposed approach can be extended to a variety of humanoid robot movements. Although the scheme is derived based on an off-line process, on-line implementation can also be accomplished. This can be done by computing the trajectory of one segment of the desired snapshots in advance, then during the execution, the segment can be further divided into several secondary segments. Thus, balance can be maintained in close to realtime through further adjustment of the secondary segments.

References

1. H. Miura and I. Shimoyama, "Dynamic walking of a biped," *The International Journal of Robotics Research*, vol. 3, no. 2, Summer 1984.
2. Y. Zheng and J. Shen, "Gait synthesis for the sd-2 biped robot to climb sloping surface," *IEEE Transactions on Robotics and Automation*, vol. 6, no. 1, pp. 86–96, Feb 1990.
3. S. Kajita, "Dynamic walking control of a biped robot along a potential energy conserving orbit," *IEEE Trans. On Robotics and Automation*, vol. 8, no. 4, pp. 431–438, 1992.
4. J. Yamaguchi, A. Takanishi, and I. Kato, "Development of a biped walking robot compensating for three-axis moment by trunk motion," in *IEEE/RSJ International Conference on Intelligent Robots and Systems*, vol. 1, July 1993, pp. 561–566.
5. J. Yamaguchi, E. Soga, S. Inoue, and A. Takanishi, "Development of a bipedal humanoid robot-control method of whole body cooperative dynamic biped walking," in *IEEE International Conference on Robotics and Automation*, vol. 1, 1999, pp. 368–374.
6. Y. Fujimoto and A. Kawamura, "Proposal of biped walking control based on robust hybrid position/force control," in *IEEE International Conference on Robotics and Automation*, 1996, pp. 2724–2730.
7. K. Nagasaka, H. Inoue, and M. Inaba, "Dynamic walking pattern generation for a humanoid

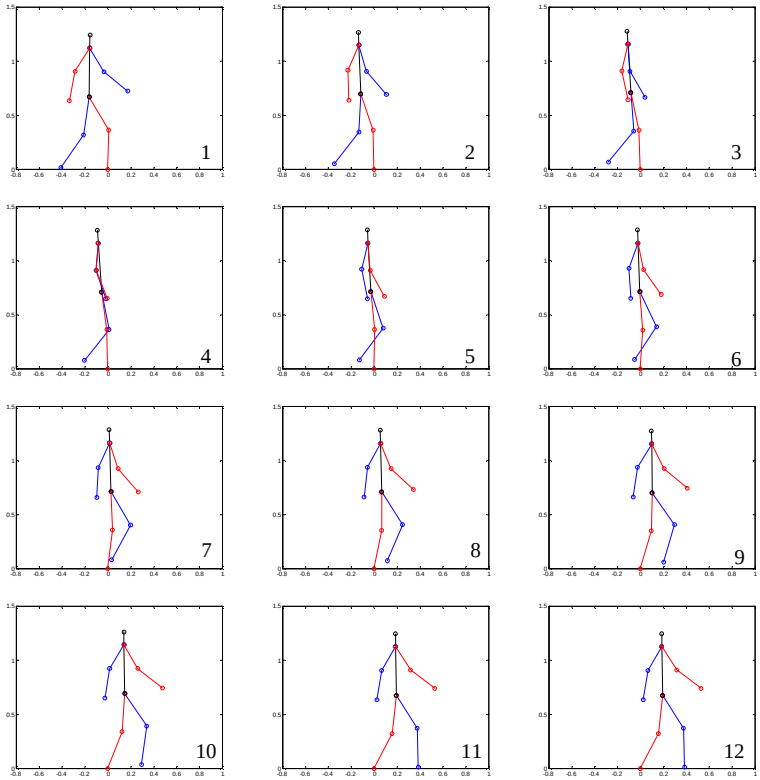

Fig. 10. Simulation results of a humanoid robot walking at a speed of one step per second. The snapshots were taken every 71.4 ms and numbered from 1 to 12.

robot based on optimal gradient method," in *IEEE SMC '99 Conference Proceedings Systems, Man, and Cybernetics*, vol. 6, 1999, pp. 908–913.

8. Q. Huang, K. Yokoi, S. Kajita, K. Kaneko, H. Arai, N. Koyachi, and K. Tanie, "Planning walking patterns for a biped robot," *IEEE Trans. on Robotics and Automation*, vol. 17, no. 3, pp. 280–289, June 2001.
9. H. O. Lim, Y. Kaneshima, and A. Takanishi, "Online walking pattern generation for biped humanoid robot with trunk," in *IEEE International Conference on Robotics and Automation*, vol. 3, 2002, pp. 3111–3116.
10. M. Vukobratovic, A. A. Frank, and D. Juricic, "On the stability of biped locomotion," *IEEE Transaction On Bio-Medical Engineering*, vol. 17, no. 1, pp. 25–26, January 1970.
11. M. Popovic, A. Hofmann, and H. Herr, "Angular momentum regulation during human walking: Biomechanics and control." IEEE International Conference on Robotics and Automation, April 2004, pp. 2405–2411.